Available online at www.sciencedirect.com
ScienceDirect
Ceramics International 35 (2009) 2831–2836
CERAMICS INTERNATIONAL
www.elsevier.com/locate/ceramint

Fabrication of 2D C/ZrC–SiC composite and its structural evolution under high-temperature treatment up to 1800 °C

Houbu Li *, Litong Zhang, Laifei Cheng, Yiguang Wang

National Key Laboratory of Thermostructure Composite Materials, Northwestern Polytechnical University, Xi'an 710072, China

Received 29 January 2009; received in revised form 1 February 2009; accepted 17 March 2009
Available online 15 April 2009

Abstract

Two-dimensional C/ZrC–SiC composites were fabricated by chemical vapor infiltration (CVI) process combined with a modified polymer infiltration and pyrolysis (PIP) method. Two kinds of ZrC slurries (ZrC aqueous slurry and ZrC/polycarbosilane slurry) were employed to densify composites before the PIP process. The as-produced C/ZrC–SiC composites exhibited better mechanical properties than the C/SiC composites densified only by CVI and PIP process. Structural evolution for C/ZrC–SiC composites treated in the range 1200–1800 °C mainly consisted of the change of SiC whiskers and the decomposition of polymer derived ceramic.

Keywords: A. Precursors: organic; B. Composites; B. Whiskers; Structural evolution

1. Introduction

Carbon fiber reinforced silicon carbide matrix composites (C_f/SiC) have been proposed as advanced materials suitable for aerospace and gas turbine engine parts, because of their potential to exhibit damage tolerance, high strength, and high stiffness [1,2].

Particularly, the oxidation resistance of C/SiC is much better than that of C/C composites because of the formation of protective silica oxide layer at temperatures below 1700 °C [3]. However, with the speed of advanced space vehicles becoming faster and faster, the temperature on surface of the nosetip or the leading edges will be over 1800 °C. C/SiC composites cannot withstand ablation environment with high heat flux and high pressure gas flow any more at such high temperatures. In our previous study, it was found that application of ablation-resistant coatings for the composites could highly improve their ablation resistance at ultrahigh temperatures (>1800 °C) [4]. However, the results also revealed that refractory particle addition (such as ZrB_2 powder) in the SiC matrix did not result in significant improvement in ablation resistance because of a large porosity (20%) of composite. Thus, it is necessary to develop a cost-effective process with the aim to highly densify the composites, and if possible, to further increase ablation resistance of the composites.

Various techniques such as chemical vapor infiltration (CVI) [5], slurry infiltration (SI) [6], polymer impregnation and pyrolysis (PIP) [7], or liquid silicon infiltration (LSI) [8] have been utilized to realize the densification of C/SiC composites. However, some of the processes have obvious disadvantages such as time-consuming, high-cost and reduction in strength for the obtained component at elevated temperatures [9]. Consequently, hybrid combined processes, whose elemental processes compensate for mutual weak points, now being well studied [9–11]. Especially, the joint of CVI, PIP and SI methods is more preferable due to its cost effectiveness and simplicity [10,12,13]. In these cases, the following major problem is found: only a limited amount powder (such as SiC powder) can be added to the polymer because of the need to keep a low slurry viscosity to reach a satisfactory impregnation efficiency [9,12]. Moreover, the low-density amorphous pyrolysis products are converted to the crystalline state at temperatures above 1400 °C, which makes precise microstructure control of ceramic matrix composites (CMCs) difficult to achieve [14]. Thus, introducing more powder into the composites and understanding the structural evolution of the polymer derived matrix become the urgent issues.

* Corresponding author. Tel.: +86 29 88486068x834; fax: +86 29 88494620.
E-mail address: houbuli@gmail.com (H. Li).

0272-8842/$36.00
doi:10.1016/j.ceramint.2009.03.030

On the basis of the previous experience, the present work aims to develop a hybrid technique to fabricate two-dimensional (2D) C/ZrC–SiC composites. The manufacturing process combines a CVI run for perform shaping and partial pre-densification, slurry infiltration and polymer impregnation–pyrolysis for matrix densification. The process described here provides a promising way to fabricate CMCs with a low final porosity and reduced process time and costs. Furthermore, surface morphologies of C/ZrC–SiC composite treated at higher temperatures are also studied to investigate its structural evolution.

2. Experimental procedure

2.1. Preparation of slurry

Two kinds of slurries, ZrC aqueous slurry and ZrC/polycarbosilane slurry, were prepared in this study. Commercially available ZrC powder (Beijing Mountain Technical Development Center, Beijing, China) with an average particle size of 1 μm (purity: 99.9%) was employed. Poly(ethylenimine) (PEI, Hengda Surface Finishing Technology Co. Ltd., Guangzhou, China; molecular weight (M_W): 10,000) and deionized water were used for the preparation of aqueous slurry. The liquid highly branched polycarbosilane (HBPCS) with allyl groups was synthesized in the Advanced Materials Laboratory at Xiamen University [15].

After dispersing the ZrC powder (20 wt%) in PEI aqueous solution (1.5 wt%) or PEI/HBPCS (1.5 wt%) solution, the slurry was milled for 12 h in a polyethylene bottle with SiC balls as the milling media.

2.2. Fabrication of 2D C/ZrC–SiC composites

The whole process for samples preparation is shown in Fig. 1. The preforms were prepared by stacking plain weave carbon cloths (T-300, ex-PAN carbon fiber, Torray) in a perforated graphite holder which was tightened to obtain the desired fiber volume fraction (generally 40%). A thin pyrolytic carbon layer (PyC) was deposited on the surface of the carbon fiber as the interfacial layer by chemical vapor infiltration process with C_3H_6 at 960 °C. The sample was then pretreated with a graphitization process at 1800 °C for 2 h. Some SiC matrix was deposited in the preforms by low-pressure chemical vapor infiltration (LPCVI). Details of LPCVI process were described elsewhere [16]. The purpose of this CVI-SiC was to increase preform stiffness and to prevent damages during subsequent processing. After CVI, the "green" C/SiC composite was machined and polished into specimens with a dimension of 40 mm × 5 mm × 3.5 mm. The apparent porosity, measured by the Archimedes method, was 18–23%.

The fabrication of 2D C/ZrC–SiC composites was carried out under the following two processing:

(A) The 2D C/SiC specimens were vacuum infiltrated with ZrC aqueous slurry for 1 h. Excess slurry was removed from the surface of the specimens after drying at 80 °C. Then, the samples, denoted as sample A, were densified by repeating six cycles of vacuum infiltration and pyrolysis with the pure HBPCS (no ZrC powder) as the polymer precursor.
(B) The specimens, denoted as sample B, experienced six cycles of ZrC/HBPCS slurry vacuum infiltration and pyrolysis process.

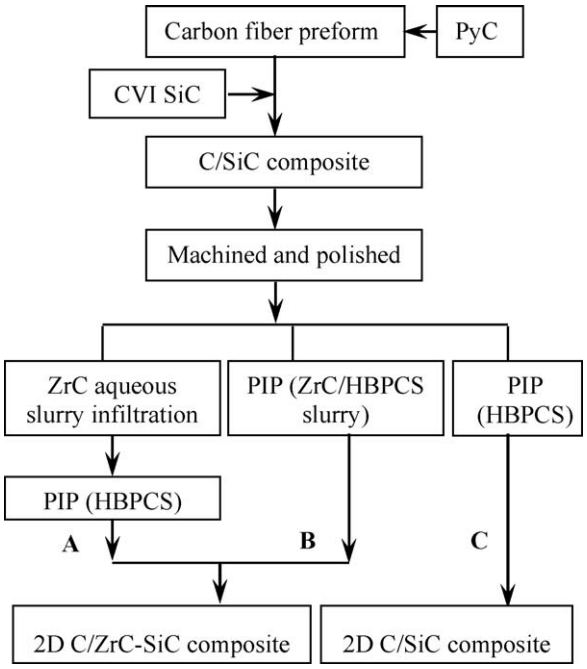

Fig. 1. Experimental procedure for preparation of 2D C/ZrC–SiC composite.

As a comparison, six cycles of PIP process were conducted on 2D C/SiC specimens by using the pure HBPCS as the pre-ceramic polymer (denoted as sample C).

In all cases mentioned above, high purity flowing argon was used as protective atmosphere with a pyrolysis temperature of 900 °C. The curing and pyrolysis process for polymer precursor were applied according to a previous study [17,18].

2.3. Characterization and heat treatment

The apparent porosity of the as-produced composites was measured by the Archimedes method. Each data point was an average of three values. Microstructure of the specimens was observed by scanning electron microscope (SEM, JSM-6700F).

Flexural strength of samples was measured by a three-point bending method, which was carried out on SANS CMT4304 machine at room temperature. The span/height ratio and cross-head speed are 15 and 0.5 mm/min, respectively. For mechanical properties tests, three specimens were measured for each composite. The C/ZrC–SiC composites after test were then heated up to 1200 °C, 1300 °C, 1400 °C, 1500 °C, 1600 °C and 1800 °C with the protection of flowing argon for 2 h, respectively. Surface morphologies of the composites were detected by SEM, while elemental analysis was conducted by energy dispersive spectroscopy (EDS).

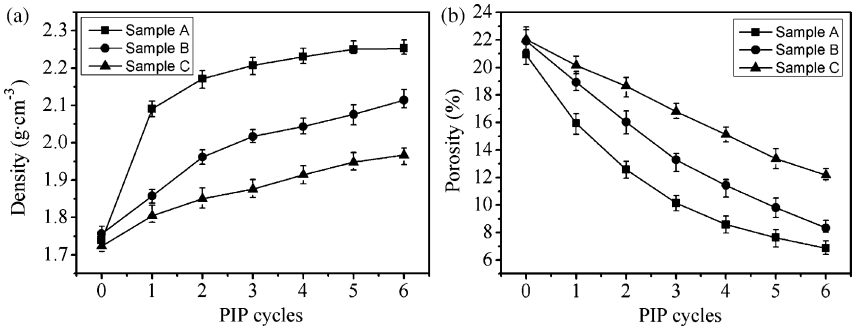

Fig. 2. Density (a) and porosity (b) versus number of PIP cycles for the preparation of three kinds of composites.

3. Results and discussion

3.1. Densification behavior and microstructure of 2D C/ZrC–SiC composite

The density and porosity change versus PIP cycles number are shown in Fig. 2. Compared with the composite densified only by PIP process (sample C), it is interesting to note that ZrC powder introduced through the slurry infiltration seems to significantly affect the subsequent PIP steps efficiently. This effect can be clearly observed in Fig. 2 where the final density and porosity change a lot, though their variation trends versus PIP cycles are similar for preforms infiltrated with and without the powder infiltration step. The ZrC powder infiltration step proved to sensibly increase the preforms density, allowing final lower porosity levels than the samples produced only by CVI and PIP.

Moreover, as shown in Fig. 2b, the porosity decreases versus PIP cycles number for the composites A and B gives an evidence to illustrate that, compared with process B, procedure A exhibits higher efficiency to densify the composite. Since the viscosity of ZrC aqueous slurry is much lower than that of ZrC/HBPCS slurry, the impregnation efficiency for the sample A is higher than that of sample B at the first stage. Then, compared with the pure HBPCS, ZrC/HBPCS slurry is not in favor of the subsequent impregnation, which results in the lower porosity decrease.

Fig. 3 shows cross-sections of the as-produced composites. As shown in Fig. 3c, some isolated large voids and cracks could be observed in the inter-bundle areas even after six infiltration–pyrolysis cycles (sample C). It is attributed to the shrinkage of the infiltrated HBPCS on pyrolysis and the difficulty for achieving effective polymer infiltration after the matrix was formed.

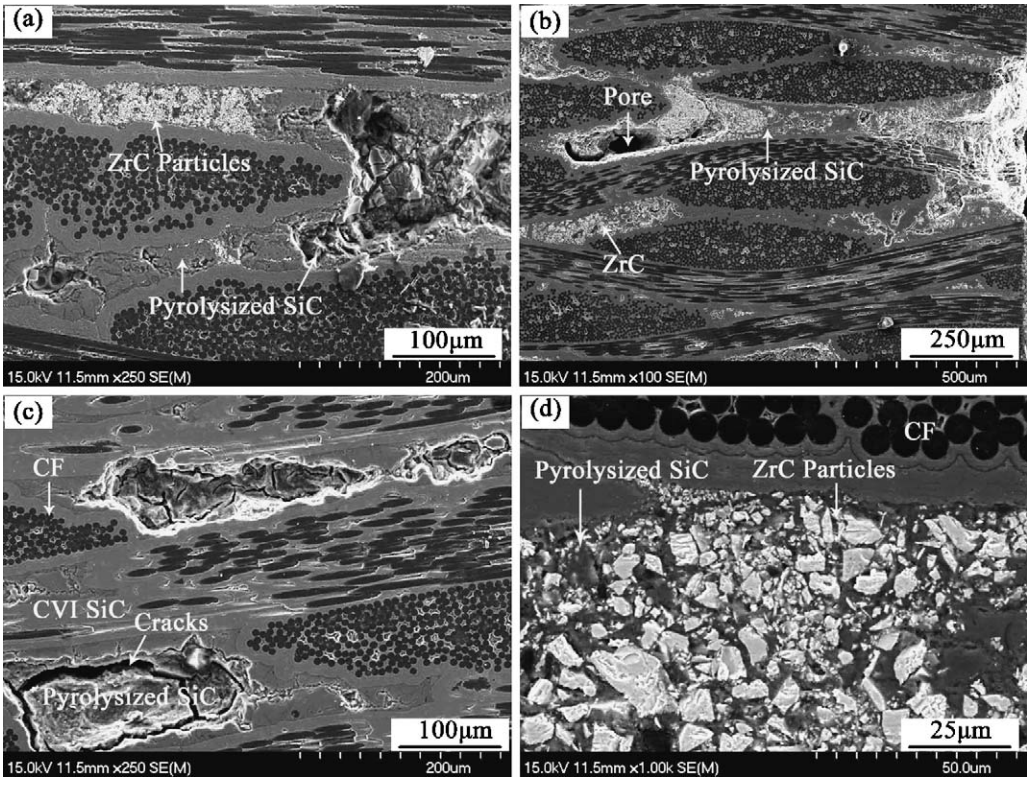

Fig. 3. Cross-sections of the as-produced composites: (a) sample A, (b) sample B, (c) sample C, and (d) larger magnification.

For the composites fabricated by powder infiltration, it can be seen that there are still a few pores in the composite (Fig. 3a and b). ZrC slurry prefers to fill large pores between the fiber bundles. During the PIP process, the liquid PCS will fill surrounding both the CVD SiC matrix and the ZrC particles. After pyrolysis, the derived SiC integrates ZrC particles in the composites (Fig. 3d). Hence, channels from the surface to the inner of composite can be easily blocked by ZrC and pyrolysized SiC. Further infiltration of the slurry thus becomes much more difficult after several PIP cycles. In addition, microstructure comparison between the composites fabricated by powder infiltration and those densified only by PIP process evidences that the ZrC powder fill effectively the large inter-bundle voids of the preforms. Furthermore, the presence of a continuous network of ZrC powder greatly reduced the length and the size of the cracks induced by the polymer shrinkage on pyrolysis (Fig. 3d).

The pyrolysized SiC and ZrC particles are relatively concentrated in samples A (Fig. 3a), while the polymer derived SiC integrates the ZrC particles more homogenous for samples B (Fig. 3b). It seems well in accordance with the different manufacturing process. For samples A, ZrC particles and HBPCS are introduced separately, while the densification media for sample B is the ZrC/HBPCS slurry.

3.2. Mechanical property of the as-produced composites

Typical stress–displacement curves derived from the bending test for the as-produced composites are shown in Fig. 4. For all the specimens, curves show an initial quasi-linear elastic region before attainment of the maximum fracture stress, followed by a continuous stress decrease. In the PIP-derived composite (samples C), the density is relatively low and the polymer derived ceramic matrix is loosely formed. Cracks will easily propagate along the weak region, and leads to fiber debonding from the matrix and then fiber pullout. It is the reason why samples C have the lowest bending strength (355 ± 20 MPa) among the three kinds of composites.

For the composites A and B which infiltrated with ZrC powder, curves (a) and (b) show that an initial quasi-linear elastic region is followed by an increasing nonlinear stress up to a maximum. Both of them exhibit a pseudo-ductile fracture behavior. After reaching the maximum value, the stress decreases gradually. However, the stress for composites C decreases directly after the initial quasi-linear elastic region (Fig. 4c) without any increasing nonlinear stress. It is revealed that the composite infiltrated with slurry displays not only higher failure stress but also better fracture toughness. As we know, the formed matrix and the interface influence the mechanical properties of the composites. For all kinds of the as-produced composites, the thickness of CVI-SiC on the outside of the fiber bundles is about 20 μm. Thus, the effect of interface on mechanical properties for all the composites is the same. Actually, the higher bending strength for samples infiltrated with ZrC particles may be attributed to the relatively densely formed matrix. The bending strength of samples A (428 ± 15 MPa) higher than that of samples B (401 ± 26MPa), further testifies the influence of a dense matrix on the mechanical properties of composites. Meanwhile, the infiltrated ZrC particles also act as reinforcement, which is beneficial for load transfer and leads to increased mechanical properties of the PIP-derived matrix. Thus, the failure stress of the final composite with the denser matrix is enhanced.

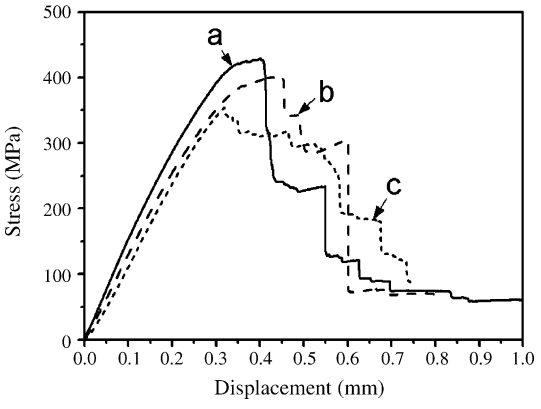

Fig. 4. Stress–displacement curves of the as-produced composites: (a) sample A, (b) sample B, and (c) sample C.

3.3. Microstructure evolution under the high-temperatures treatment

Fig. 5a shows the surface morphology of 2D C/ZrC–SiC composite heat-treated at 1200 °C. It can be clearly seen that the intrinsic shrinkage during polymer–ceramic conversion process results in large amount of cracks. ZrC particles are embedded in the polymer derived SiC ceramics. In addition, the surface of the sample is partially covered with whiskers. The whiskers are generally several micrometers in length and nanometers in diameter, and randomly oriented with straight morphology. A spherical part is observed on the tip of each whisker. EDS analysis (Fig. 6a) reveals that the spherical part contains iron and nickel. Only the Si and C elements are detected (Fig. 6b) in the center of the whiskers, indicating a pure Si–C chemistry in whiskers. Both the pyrolysized SiC ceramic and the ZrC powder are thought to contain impurities such as iron and nickel. According the Fe–Ni phase graph, iron and nickel can form low-melting point eutectic alloy at low temperature. Whisker nucleation can occur on such alloys [19]. The spherical part which contains Fe–Ni alloy on the tip of the whisker implies that the whisker is formed by vapor–liquid–solids (VLSs) mechanism [19–21]. The growth morphology of the whiskers at different heat-treating temperatures in Fig. 5 testified the growth process.

At 1200 °C, nanosized spherical particles and short whiskers with length lower than 200 nm are observed on the surface of the composite. Each of them has a spherical part in the tip. It can be deduced that the Fe–Ni catalyst liquid droplets were formed below 1200 °C. As we know, HBPCS derived SiC ceramic has a microstructure which is composed of β-SiC crystallites, free carbon and amorphous oxycarbide (SiC_XO_Y) [18,22]. The SiC_XO_Y phase which is unstable at such a temperature

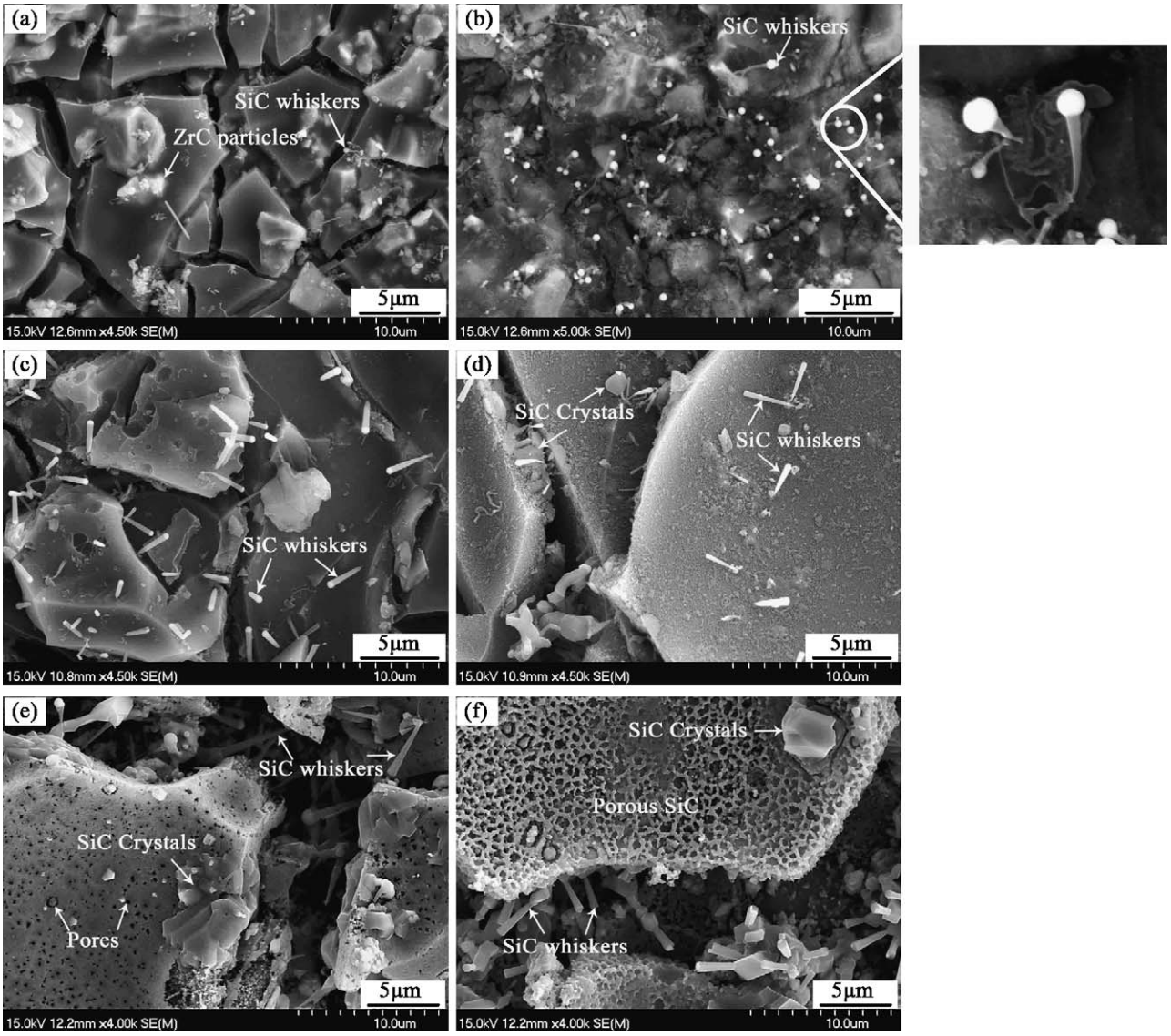

Fig. 5. Surface morphologies of 2D C/ZrC–SiC composite heat-treated at: (a) 1200 °C, (b) 1300 °C, (c) 1400 °C, (d) 1500 °C, (e) 1600 °C, and (f) 1800 °C.

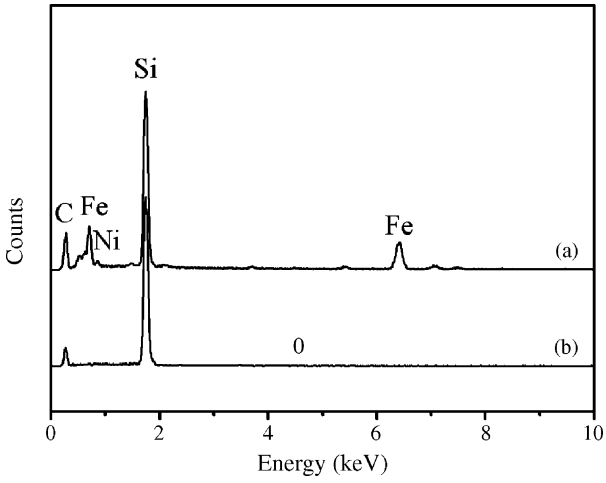

Fig. 6. EDS for (a) the tip of the whisker and (b) the center of the whisker.

decomposes to β-SiC crystals by evolving SiO and CO gases [22,23]:

$$SiC_XO_Y(s) \rightarrow SiC(s) + SiO(g) + CO(g) \quad (1)$$

Then, the SiO and CO gas dissolve into liquid droplets to form β-SiC nanocrystal [22–24]:

$$SiO(g) + 3CO(g) \rightarrow SiC(s) + CO_2(g) \quad (2)$$

As the temperature increased, the concentration of β-SiC nanocrystal is supersaturated in the catalyst liquid droplets, which grows along the thermodynamically favorable direction to form whiskers at the solid–liquid interface [19]. As the heat-treating temperatures gradually increase, the whiskers grow and become longer. At 1300 °C (Fig. 5b) and 1400 °C (Fig. 5c), a large amount of whiskers with straight shape has been formed, and all of them also have spherical part at the tips.

Fig. 5d–f shows the surface morphologies of the composites heat-treated at 1500 °C, 1600 °C and 1800 °C, respectively. The

whiskers have no spherical part, and iron and nickel are not detected at the tip of the whiskers. The results suggest that the spherical parts have been evaporated from the tips of the whiskers. Therefore, it can be assumed that the growth process of whiskers changes from VLS to VS as the heat-treating temperature increased to 1500 °C [19,25]. Then, as the temperature increased, the whiskers become longer and broader.

On the other hand, such high-temperature treatments cause changes in the microstructure of the polymer derived ceramic, that is, the coarsening of β-SiC crystallites and the production of imperfections such as pores and flaws (Fig. 5e). The polymer derived SiC showed a porous microstructure and larger grains deposition on the ceramic surface, when heat-treated at 1600 °C (Fig. 5e) and 1800 °C (Fig. 5f). The large bulk crystals deposited on the ceramic surface are the β-crystals which were produced according to the gas-phase reaction (2) and the following reaction [26]:

$$\mathrm{SiO(g)} + 2\mathrm{C(s)} \rightarrow \mathrm{SiC(s)} + \mathrm{CO(g)} \quad (3)$$

EDS analysis for the whole composite heat-treated at different temperatures displays the gradual decrease in oxygen content, further testifies the decomposition of amorphous SiC_XO_Y ceramic. The formation of porous structure in ceramic could be attributed to the rapid evolution of gases at the earlier stage of high-temperature exposure according to reaction (1). Additionally, from the overall analysis, ZrC powder seems to have little influence on the structural evolution of the as-produced composites.

4. Conclusions

In conclusion, 2D C/ZrC–SiC composites were fabricated by a combined process of CVI/SI/PIP. In order to introduce ZrC powder into the composite, two kinds of slurries were employed: ZrC aqueous slurry and ZrC/polycarbosilane slurry. The process for composites densification by infiltrating ZrC aqueous slurry before the PIP process exhibited higher efficiency. The as-produced C/ZrC–SiC composites by such process possessed not only a somewhat higher bending strength, but also a better toughness. Morphologies evolution for C/ZrC–SiC composites treated in the range of 1200–1800 °C consists in the formation of SiC whiskers and the decomposition of the polymer derived ceramic. Further decomposition of the HBPCS derived ceramic together with impurities in ceramic and ZrC powder gave rise to the evolution of SiC whiskers.

References

[1] T.M. Besmann, B.W. Sheldon, R.A. Lowden, D.P. Stinton, Vapor phase fabrication and properties of continuous filament ceramic composites, Science 253 (6) (1991) 1104–1109.
[2] S. Schmidt, S. Beyer, H. Knabe, H. Immich, R. Meistring, A. Gessler, Advanced ceramic matrix composite materials for current and future propulsion technology applications, Acta Astronaut. 55 (2004) 409–420.
[3] J.R. Strife, J.E. Sbeehan, Ceramic coatings for carbon–carbon composites, Am. Ceram. Soc. Bull. 67 (2) (1988) 369–374.
[4] H.B. Li, L.T. Zhang, L.F. Cheng, Y.G. Wang, Ablation resistance of different coating structures for C/ZrB_2–SiC composites under oxyacetylene torch flame, Int. J. Appl. Ceram. Technol. 6 (2) (2009) 145–150.
[5] Y.D. Xu, L.F. Cheng, L.T. Zhang, H.F. Yin, X.W. Yin, Mechanical properties of 3D fiber reinforced C/SiC composites, Mater. Sci. Eng. A 300 (2001) 196–202.
[6] S. Lee, M. Weinmann, F. Aldinger, Fabrication of fiber-reinforced ceramic composites by the modified slurry infiltration technique, J. Am. Ceram. Soc. 90 (8) (2007) 2657–2660.
[7] M. Berbon, M. Calabrese, Effect of 1600 °C heat treatment on C/SiC composites fabricated by polymer infiltration and pyrolysis with allylhydridopolycarbosilane, J. Am. Ceram. Soc. 85 (7) (2002) 1891–1893.
[8] R. Kochendörfer, Low cost processing for C/C–SiC composites by means of liquid silicon infiltration, Key Eng. Mater. 164–165 (1999) 451–456.
[9] S.R. Zbigniew, A Process for C_f/SiC composites using liquid polymer infiltration, J. Am. Ceram. Soc. 84 (10) (2001) 2235–2239.
[10] K. Suzuki, S. Kume, K. Nakano, T.W. Chou, Fabrication and characterization of 3D C/SiC composites via slurry and PCVI joint process, Key Eng. Mater. 164–165 (1999) 113–116.
[11] Y.Z. Zhu, Z.G. Huang, S.M. Dong, M. Yuan, D.L. Jiang, Manufacturing 2D carbon-fiber-reinforced SiC matrix composites by slurry infiltration and PIP process, Ceram. Int. 34 (5) (2008) 1201–1205.
[12] C.A. Nannetti, A. Ortona, D.A. Pinto, B. Riccardi, Manufacturing SiC-fiber reinforced SiC matrix composites by improved CVI/slurry infiltration/polymer impregnation and pyrolysis, J. Am. Ceram. Soc. 87 (7) (2004) 1205–1209.
[13] K. Suzuki, K. Nakano, S. Kume, T.W. Chou, Fabrication and characterization of 3D carbon fiber reinforced SiC matrix composites via slurry and pulse–CVI joint process, Ceram. Eng. Sci. Proc. 19 (3) (1998) 259–266.
[14] E. Kroke, Y.L. Li, C. Konetschny, E. Lecomte, C. Fasel, A. Riedel, Silazane delivered ceramics and related materials, Mater. Sci. Eng. 26 (4–6) (2000) 97–199.
[15] T.H. Huang, Z.J. Yu, X.M. He, M.H. Huang, L.F. Chen, H.P. Xia, L.T. Zhang, One-pot synthesis and characterization of a new, branched polycarbosilane bearing allyl groups, Chin. Chem. Lett. 18 (2007) 754–757.
[16] L.F. Cheng, Y.D. Xu, L.T. Zhang, X.W. Yin, Oxidation behavior of three dimensional C/SiC composites in air and combustion gas environments, Carbon 38 (2000) 2103–2108.
[17] H.B. Li, L.T. Zhang, L.F. Cheng, Y.G. Wang, Z.J. Yu, M.H. Huang, H.B. Tu, H.P. Xia, Effect of the polycarbosilane structure on its final ceramic yield, J. Eur. Ceram. Soc. 28 (2008) 887–891.
[18] H.B. Li, L.T. Zhang, L.F. Cheng, Y.G. Wang, Z.J. Yu, M.H. Huang, H.B. Tu, H.P. Xia, Polymer–ceramic conversion of a highly branched liquid polycarbosilane for SiC-based ceramics, J. Mater. Sci. 43 (2008) 2806–2811.
[19] X.M. Yao, S.H. Tan, Z.G. Huang, S.M. Dong, D.L. Jiang, Growth mechanism of β-SiC nanowires in SiC reticulated porous ceramics, Ceram. Int. 33 (2007) 901–904.
[20] G. Mcmahon, G.J.C. Carpenter, T.F. Malis, On the growth mechanism of silicon carbide whiskers, J. Mater. Sci. 26 (1991) 5655–5663.
[21] J.V. Milewski, F.D. Gac, J.J. Petrovic, S.R. Skagg, Growth of beta-silicon carbide whiskers by the VLS process, J. Mater. Sci. 20 (1985) 1160–1166.
[22] T. Shimoo, K. Okamura, M. Ito, M. Takeda, High-temperature stability of low-oxygen silicon carbide fiber heat-treated under different atmosphere, J. Mater. Sci. 35 (2000) 3733–3739.
[23] T. Shimoo, I. Tsukada, T. Seguchi, K. Okamura, Effect of firing temperature on the thermal stability of low-oxygen silicon carbide fibers, J. Am. Ceram. Soc. 81 (8) (1998) 2109–2115.
[24] J.J. Sha, T. Hinoki, A. Kohyama, Microstructural characterization and fracture properties of SiC-based fibers annealed at elevated temperatures, J. Mater. Sci. 42 (2007) 5046–5056.
[25] S. Otoishi, Y. Tange, Growth rate and morphology of silicon carbide whiskers from polycarbosilane, J. Cryst. Growth 200 (1999) 467–471.
[26] M. Takeda, J. Sakamoto, Y. Imai, H. Ichikawa, Thermal stability of the low-oxygen-content silicon carbide fiber Hi-Nicalon™, Compos. Sci. Technol. 59 (1999) 813–819.